

The Role of Laser Field Effect on Thermo-Spin Transport Properties through Serially Coupled Quantum Dots System

Zainab A. Abd AL-Ridha^{1,*}, Salah A. H. Al Murshidee¹, and Rasha A. Hussein¹

¹ Department of Physics, College of Science, Al Muthanna University, Muthanna, Iraq

*Corresponding Author: Sci.zainabak@mu.edu.iq

Received 12 June. 2025, Accepted 2 Oct. 2025, published 30 Dec. 2025.

DOI: 10.52113/2/12.02.2025/90-100

Abstract: An analytical model of serially configuration coupled quantum dots system consisting of two splitting spin strongly hybrid with two normal leads (electrodes) is proposed to investigate the role of laser field on the thermos-spin tunneling properties, Anderson model are utilized, duo to Coulomb correlation between the two splitting spin energy levels in each quantum dot. The occupation numbers on each quantum dot are formulated and solved it self-consistently. The solutions are then used to evaluate the spin currents and the differential conductance. The calculations declare that the total spin current become enhanced when coupling interaction (V_{12}) increases, and the spin differential conductance show two splitting peaks separated by conductance gap which reflects the Pauli-spin blockade, the energy spacing between splitting peaks is equal to the value of the (V_{12}). As the value of (V_{12}) increases the spin conductance gap decreases. When the laser field interact with each quantum dot, the spin differential conductance enhances and induces the photon-assisted (FAT) peaks in differential conductance spectrum. An interesting results is the observation of photon-assisted (FAT) peak that can be emerged in the Pauli-spin blockade effects around ($\Delta u = 0$) region especially when $V_{12} = \hbar\omega = 0.04eV$.

Keywords: Quantum dots, Double Quantum dot, Spintronic, thermospin, Nanoelectronics devices.

1. Introduction

One of the most important goal in nanoscale systems is to understand, and control electrical, spin and heat tunneling through the system consist of two splitting spin double coupled quantum dots in highly controlled conditions [1].

Artificially coupled double quantum dot systems have attracted significant interest in both theoretical and experimental research

due to their ability to regulate charge, spin current and heat flow within the system [2, 3]. Spin tunneling through artificial double quantum dot molecules (double quantum dots coupled serially) is strongly affected by Coulomb interaction, Pauli spin blockade (P.SB) and the coupling interaction between double quantum dots (DQD) [4]. The role between Pauli spin blockade (P.SB) and Coulomb interaction can be exploited to

suppress current flow in one side while allowing it in the opposite. Under such conditions, double quantum dots (DQDs) may function as tunable Spin-Coulomb rectifiers, making them promising candidates for spintronic applications such as spin-based memory elements and transistors.

[5]. Moreover, the double quantum dots (DQD) system shows some novel physical properties, including quantum Hall effect, Kondo effect, Fano effect, thermoelectric effect and Photon-assisted tunneling effect (FAT) [6]. The (FAT) has attracted more attention in recent years due to potential application in photoelectron and quantum computing devices [7-9]. When photon experiences on quantum dot (QD), the (FAT) effect emerges in the induced photon-current in system consist of quantum dots (QDs) embedded between two leads [10], in order to understand this physical phenomenon, many different methods had introduced such as nonequilibrium Green function(NEGF) method, transfer Hamiltonian approach and the nonequilibrium Green's function formalism based on Keldysh theory [8,10]. One of the most important features of quantum dot system is its ability to allow energy exchange between the electron and the externally applied field, leading to a new tunneling channels, rustling an additional

peak that emerge in the Coulomb blockade reign, this added phenomenon can be linked to the (FAT) [10, 11]. Quantum dot (QD) systems are important for studying quantum effects in thermos-spin transport such as the spin Seebeck effect, when a thermal gradient that is applied to the system's various ends emerges Seebeck effect. The spin Seebeck effect, produces pure spin current in the absence of an associated charge current or spin bias, the latter being characterized by a difference in the chemical potentials of spin-up and spin-down electrons. It makes it possible to use the extra heat produced by nanostructures to increase thermal device performance and reduce energy consumption. This emerging phenomenon provides an alternative method for manipulating electron spin and holds potential for direct application in the development of thermal spin generators used to power spintronic devices. [12-14].

In this study an extended model calculation was presented to examine the impact laser field on thermos-spin transport in a device consists of two serially coupled double quantum dots (which have considered as artificial molecule), attached to normal metallic electrodes (i.e. left and right leads). Our model is based on two impurity Anderson model for serially coupled two atoms chemisorbed on solid surface.

2. The Mathematical Model

The two impurity Anderson model is utilized to model the role of laser filed on system consist of two serially coupled DQD embedded between normal metallic electrodes, and supposing there are only two splitting energy levels in each QD_i , results from Coulomb correlation. The system considered in this study can be given by the following Hamiltonian [15, 4]: -

$$H = H_{DQD} + H_{leads} + H_{DQD-leads} + H_{QD-QD} \quad (1)$$

Where

$$H_{DQD} = \sum_{\sigma} \sum_{i=1}^2 E_i^{\sigma} n_{i\alpha}^{\sigma} + \sum_{i=1}^2 U_i n_{i\alpha}^{\sigma} n_{i\alpha}^{-\sigma},$$

is the Hubbard Hamiltonian of the DQD system, with

$$E_1^{\pm\sigma} = E_1 + U_1 n_{1L}^{\mp\sigma} - J n_{2R}^{\pm\sigma} \text{ and}$$

$$E_2^{\pm\sigma} = E_2 + U_2 n_{2R}^{\mp\sigma} - J n_{1L}^{\pm\sigma},$$

represents the QD_i energy level with spin σ , E_i is the QD_i effective energy level and U_i , describes the Coulomb energy between the two splitting energy level in QD_i . $n_{i\alpha}^{\sigma}$ is the occupation numbers of QD_i and $C_i^{\sigma+}$ (C_i^{σ}) represents the creation (annihilation) operator on the splitting energy level E_i^{σ} .

$H_{leads} = \sum_{\sigma} \sum_{\alpha} \sum_{k_{\alpha}} E_{k_{\alpha}}^{\sigma} C_{k_{\alpha}}^{\sigma+} C_{k_{\alpha}}^{\sigma}$ describes the Hamiltonian of the normal metallic electrodes, where $C_{k_{\alpha}}^{\sigma+}$ ($C_{k_{\alpha}}^{\sigma}$) represents the electron creation (annihilation) operator in the normal metallic

electrode (α), with energy $E_{k_{\alpha}}^{\sigma}$.

$$H_{DQD-leads} = \sum_{\sigma} \sum_{\alpha} \sum_{i=1}^2 \sum_{k_{\alpha}} (V_{ik_{\alpha}} C_i^{\sigma+} C_{k_{\alpha}}^{\sigma} + H.C.),$$

is the Hamiltonian describes the interaction between the QD_i and the normal metallic electrodes (leads) α , where $V_{ik_{\alpha}}$ describes the matrix elements of the QD_i that strongly coupled with the normal metallic electrode α .

The last Hamiltonian

$$H_{QD-QD} = \sum_{\sigma} [(V_{12} C_1^{\sigma+} C_2^{\sigma} + H.C.) + \frac{1}{2} J (C_1^{\sigma+} C_2^{\sigma+} C_1^{\sigma} C_2^{\sigma} + H.C.)]$$

, describes QD-QD coupling interaction, J

represents exchange interaction, where (H.C.)

denotes the Hermitian conjugate. The occupation

numbers n_i^{σ} can be given by the following

relation [16]:

$$n_i^{\sigma} = \sum_{n=0,\pm 1} K_n \int_{u_{0\alpha}}^{\phi_{\alpha}} \rho_{i\alpha}^{\sigma}(E) f_{\alpha}^{\sigma}(E, T) dE \quad (2)$$

$$K_0 = \frac{\Gamma_{\alpha}^{\sigma}}{\Gamma_{\alpha}^{\sigma} + 2\Gamma_{ls}} \quad , \quad K_{-1} = K_1 = \frac{\Gamma_{ls}}{\Gamma_{\alpha}^{\sigma} + 2\Gamma_{ls}}$$

Where $u_{0\alpha}$ is the band bottom chemical

potential of the normal metallic electrodes

(leads), ϕ_{α} is the work function of the normal

metallic electrode (lead) and $f_{\alpha}^{\sigma}(E, T_{\alpha})$

represents the probability function for the

normal metallic electrode α . $\rho_{i\alpha}^{\sigma} = -\frac{1}{\pi} \text{Im} G_{i\alpha}^{\sigma}(E)$ Is

the density of states on the quantum dots QD_i

that coupled strongly with the normal metallic electrode (lead) and $G_{i\alpha}^\sigma(E)$ is the Green's functions of the QD_i with spin σ , described by the following relation [17-22].

$$G_{i\alpha}^\sigma(E) = \frac{1}{2} \sum_{j=+,-} \frac{C_{ij}}{(E - E_{ij}^\sigma + n\hbar\omega) + i(\Gamma_{i\alpha}^\sigma + \Gamma_{ls})} \quad (3)$$

Where $\Gamma_{i\alpha}^\sigma(E) = 2\pi \sum_k |V_{ik\alpha}|^2 \delta(E - E_{k\alpha})$ is the broadening in the energy levels of QD_i [23-25]. Depending on the wide-band approximation, the $\Gamma_{i\alpha}^\sigma$ will be energy-independent [26-27]. Γ_{ls} , describes the broadening of the energy levels of QD_i due to laser field interaction. $E_{i\pm}^\sigma = E_i + U_i n^\mp \sigma - J n^\pm \sigma \pm V_i^\pm \sigma$, is the molecular energy levels, with $j \equiv (+, -)$, if $i = 1$ then $\alpha \equiv L$ and if $i = 2$ then $\alpha \equiv R$. Where C_{ij}^σ for different i and j described by following [15, 4]:

$$C_{1j}^\sigma = \frac{1}{2\pi} \left(1 + j \frac{K_1^\sigma}{V_1^\sigma}\right); \quad C_{2j}^\sigma = \frac{1}{2\pi} \left(1 - j \frac{K_2^\sigma}{V_2^\sigma}\right) \quad (4)$$

With $V_i^\sigma = \sqrt{V_{12}^2 + (K_i^\sigma)^2}$, $K_i^\sigma = U_i m^{-\sigma} + J m^\sigma$,

$$n^\sigma = \frac{n_1^\sigma + n_2^\sigma}{2} \text{ and } m^\sigma = \frac{n_1^\sigma - n_2^\sigma}{2}$$

The channel of the spin current flows through the active region (DQDs) can be described by the following formula [28-29].

$$I^\sigma = \frac{e}{h} \frac{\Gamma_{1L}^\sigma \Gamma_{2R}^\sigma}{\Gamma_{1L}^\sigma + \Gamma_{2R}^\sigma} \sum_{n=1,0,-1} K_n \int \rho^\sigma(E) [f_L^\sigma(E, T_\alpha) - f_R^\sigma(E, T_\alpha)] dE \quad (5)$$

We can write eq. (5) in term of occupation numbers eq. (2) as;

$$I^\sigma = \frac{e}{h} \frac{\Gamma_{1L}^\sigma \Gamma_{2R}^\sigma}{\Gamma_{1L}^\sigma + \Gamma_{2R}^\sigma} \sum_{n=1,0,-1} K [\{ (n_{1L}^\sigma - n_{2R}^\sigma) + (n_{2L}^\sigma - n_{1R}^\sigma) \}] \quad (6)$$

Based on Taylor expansion for the probability function about $E = \mu_\alpha^\sigma$, an analytical formulation was derived to calculate the $n_{i\alpha}^\sigma$ on QD_i as the following;

$$n_{i\alpha}^\sigma = \sum_{n=0,\pm 1} \sum_{j=+,-} C_{ij}^\sigma \left\{ -\tan^{-1} \left(\frac{u_{0\alpha} - (\mu_\alpha^\sigma - k_B T_\alpha) - E_{ij}^\sigma + n\hbar\omega}{\Gamma_{i\alpha}^\sigma + \Gamma_{ls}} \right) + \left[1 - M_{0\alpha j}^\sigma + M_{2\alpha j}^\sigma (\Gamma_{i\alpha}^\sigma)^2 \right] \tan^{-1} \left(\frac{\mu_\alpha^\sigma - k_B T_\alpha - E_{ij}^\sigma + n\hbar\omega}{\Gamma_{i\alpha}^\sigma + \Gamma_{ls}} \right) \right. \\ \left. + \left[M_{0\alpha j}^\sigma - M_{2\alpha j}^\sigma (\Gamma_{i\alpha}^\sigma + \Gamma_{ls})^2 \right] \tan^{-1} \left(\frac{\mu_\alpha^\sigma + k_B T_\alpha - E_{ij}^\sigma + n\hbar\omega}{\Gamma_{i\alpha}^\sigma + \Gamma_{ls}} \right) + \frac{1}{2} \left[M_{1\alpha j}^\sigma \Gamma_{i\alpha}^\sigma - M_{3\alpha j}^\sigma (\Gamma_{i\alpha}^\sigma)^3 \right] \ln \frac{(\mu_\alpha^\sigma + k_B T_\alpha - E_{ij}^\sigma + n\hbar\omega)^2 + (\Gamma_{i\alpha}^\sigma + \Gamma_{ls})^2}{(\mu_\alpha^\sigma - k_B T_\alpha - E_{ij}^\sigma + n\hbar\omega)^2 + (\Gamma_{i\alpha}^\sigma + \Gamma_{ls})^2} \right. \\ \left. + 4M_3 (\Gamma_{i\alpha}^\sigma + \Gamma_{ls}) (E_{ij}^\sigma + n\hbar\omega - \mu_\alpha^\sigma) k_B T_\alpha \right\} \quad (7)$$

Where

$$M_{0\alpha j}^\sigma = a_0 + a_1 (E_{ij}^\sigma - \mu_\alpha^\sigma) + a_3 (E_{ij}^\sigma - \mu_\alpha^\sigma)^3, \quad M_{1\alpha j}^\sigma = a_1 + 3a_3 (E_{ij}^\sigma - \mu_\alpha^\sigma)^2 \\ M_{2\alpha j}^\sigma = 3a_3 (E_{ij}^\sigma - \mu_\alpha^\sigma), \quad M_{3\alpha j}^\sigma = a_3$$

$$\text{With } a_0 = 0.5, \quad a_1 = -\frac{0.25}{k_B T_\alpha^\sigma}, \quad a_3 = \frac{0.02083333}{(k_B T_\alpha^\sigma)^3}$$

Spin current and the spin differential conductance can be described by the following [4, 30],

$$I_S = \frac{\hbar}{2} (I^\sigma - I^{-\sigma}), \quad G_{diff} = \frac{\partial I}{\partial (eV_{sb})} \quad (8)$$

With $I = I^\sigma, I^{-\sigma}, I_S$ and eV_{sb} is the spin bias applied. Notably, the spin current and the spin differential conductance will be expressed in arbitrary units.

3. Results and Discussion

The extended theoretical model was highlighted to investigate the effects of laser field on spin current and conductance through coupled quantum dots generated due to the Seebeck effect which describes the generation of a voltage as a results of temperature gradient between the left and right leads in the case

$$V_{12} > \Gamma_\alpha^\sigma, \quad \text{with} \quad \Gamma_\alpha^\sigma = 0.005eV,$$

$$\Gamma_{Laser}^\sigma = 0.003eV, E_1 = E_2 = 0.005eV,$$

$U = 0.001eV, J = 0.1eV$. For this purpose, we use temperature gradient to control the chemical potential gradient which can be also controlled by bias voltage $eV_{sb} = 0.02eV$.

In fig. (1), The total spin current I_S shows one-step behavior emerges at a certain temperature gradient polarity, the width of the step decreases as the coupling interaction (V_{12}) increases and the total spin current become enhanced. As the laser field exerted on each quantum dot directly, the step like behavior decreases, when the coupling interaction (V_{12}) increases, the step decreases more and show linear behavior in the Pauli-spin blockade effect around ($\Delta u = 0$)

region and the device behaves as resistor in this region when $V_{12} = \hbar\omega = 0.04eV$.

The spin differential conductance in fig. (2) show two splitting peaks separated by conductance gap which reflects the Pauli-spin blockade, the energy spacing between slitting peaks is equal to the value of the coupling interaction (V_{12}). As the value of (V_{12}) increases the spin conductance gap decreases. When the laser field interact with quantum dots, the spin differential conductance enhances and induces the photon-assisted (FAT) peaks in differential conductance spectrum. An interesting results is the observation of photon-assisted (FAT) peak that can be emerged in the Pauli-spin blockade effects around ($\Delta u = 0$) region especially when $V_{12} = \hbar\omega = 0.04eV$.

Fig. (3) Show the spin current as a function of the energy levels of the quantum dots. For different values of (V_{12}). In the absence of laser field, the spin current spectrum exhibit peaks in the positive values of quantum dots, while no spin current flow in the negative value due to the Pauli-spin blockade effects. When the laser field exists, the spin current spectrum enhances and induces the photon-assisted (FAT) peaks in current spectrum. An interesting result is the observation of photon-assisted (FAT) peaks that can be emerged in the negative values of the energy levels of the quantum dots.

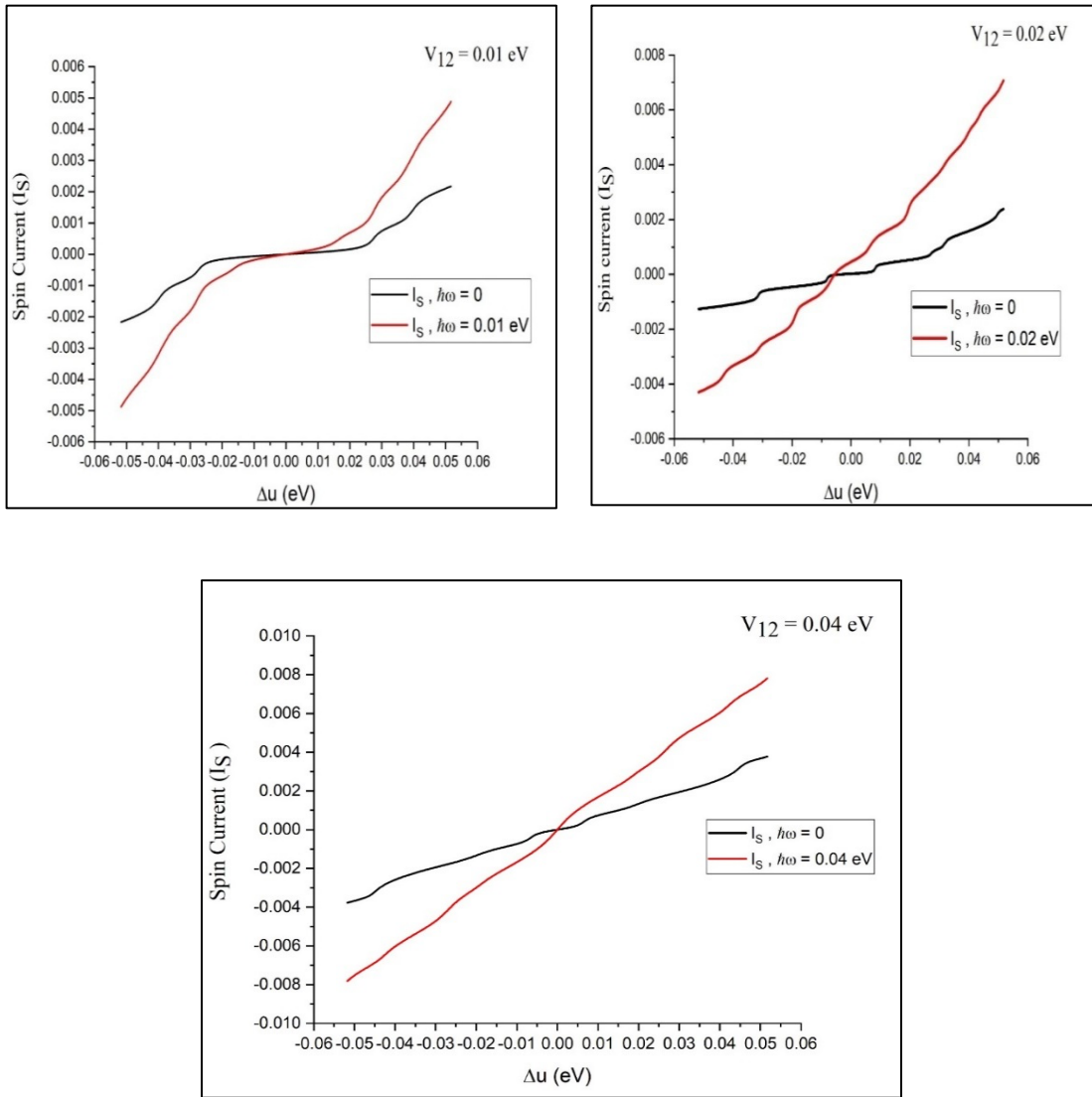


Fig.(1):The I_S as a function of temperature gradient for different values of coupling interaction, in the case of absence and presence of laser at $E_d = 0.005eV$,
 $V_{sb} = 0.02eV$, $\Gamma_{Laser}^\sigma = 0.003eV$, $\Gamma_\alpha^\sigma = 0.005eV$, $U = 0.001eV$, $J = 0.1eV$.

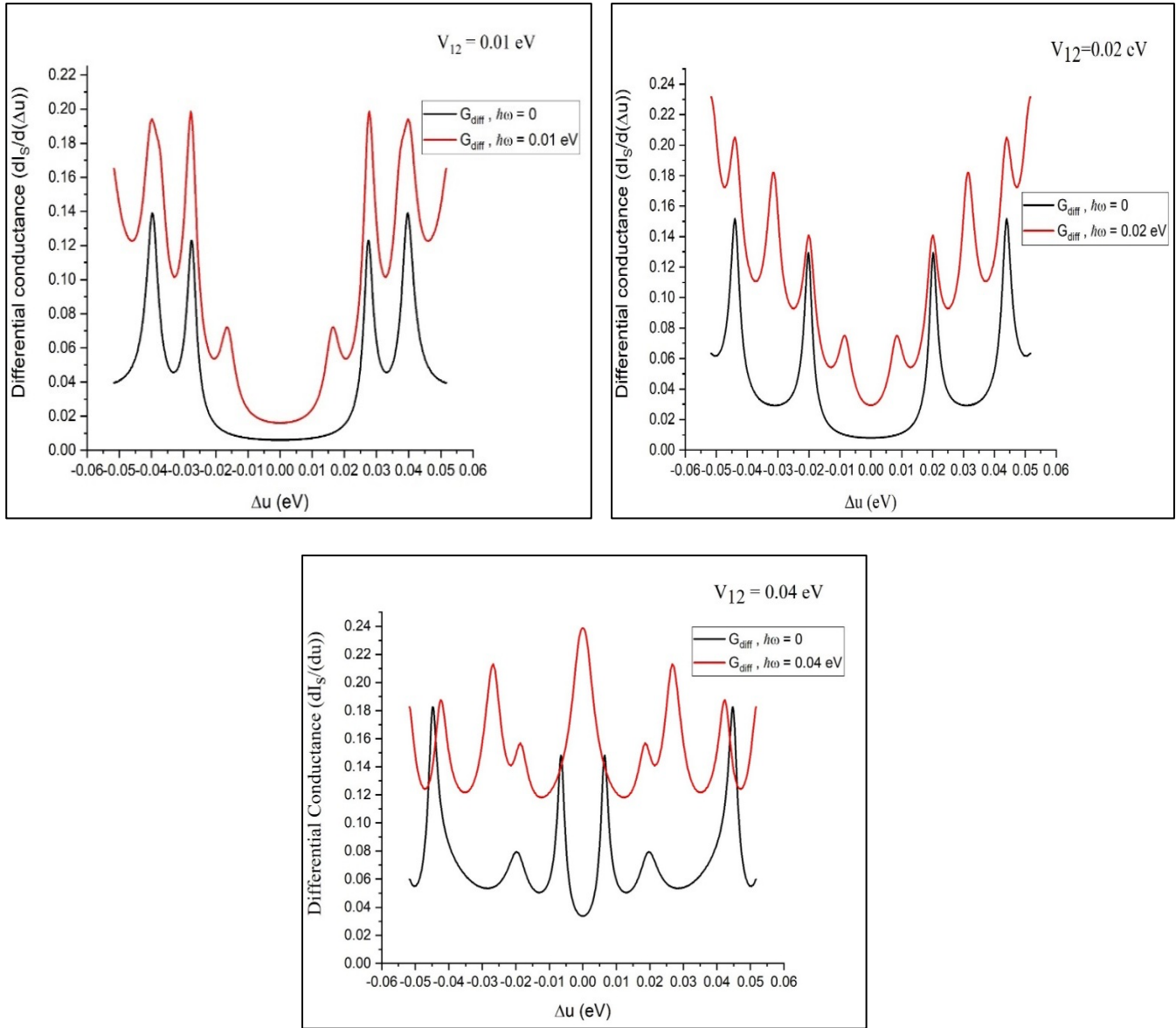


Fig. (2): The $G_{(diff)}$ as a function of temperature gradient for different values of coupling interaction, in the case of absence and presence of laser at $E_d = 0.005eV$, $V_{sb} = 0.02eV$, $\Gamma_{Laser}^\sigma = 0.003eV$,

$$\Gamma_\alpha^\sigma = 0.005eV, U = 0.001eV, J = 0.1eV.$$

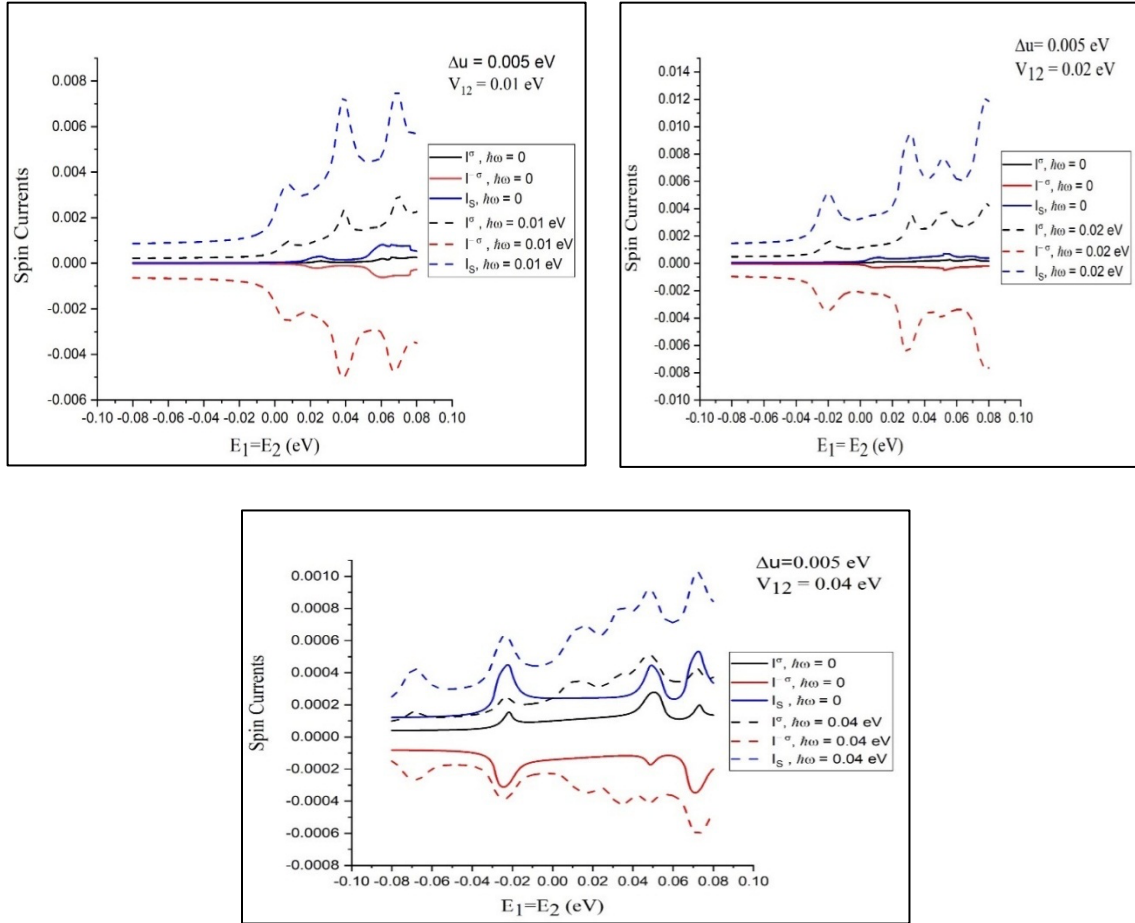


Fig.(3): The spin current channels as a function of quantum dots energy levels for different values of coupling interaction, in the case of absence and presence of laser at $E_d = 0.005eV$, $V_{sb} = 0.02eV$,

$$\Gamma_{Laser}^{\sigma} = 0.003eV, \Gamma_{\alpha}^{\sigma} = 0.005eV, U = 0.001eV, J = 0.1eV.$$

4. Conclusion

The total spin current I_S , shows one-step behavior emerges at a certain temperature gradient polarity, the width of the step decreases as the (V_{12}) increases and the total spin current become enhanced. As the laser field exerted on each quantum dot directly, the step like behavior decreases, as the coupling interaction (V_{12})

increases, the step decreases more and show linear behavior in the Pauli-spin blockade effect around ($\Delta u = 0$) region and the device behaves as resistor in this region when $V_{12} = \hbar\omega = 0.04eV$.

The spin differential conductance show two splitting peaks separated by conductance gap which reflects the Pauli-spin blockade, the energy spacing between splitting peaks is equal

to the value of the (V_{12}). As the value of (V_{12}) increases the spin conductance gap decreases. When the laser field interact with quantum dots, the spin differential conductance enhances and induces the photon-assisted (FAT) peaks in differential conductance spectrum. An interesting results is the observation of photon-assisted (FAT) peak that can be emerged in the Pauli-spin blockade effects around ($\Delta u = 0$) region especially when $V_{12} = \hbar\omega = 0.04eV$.

The tuning of quantum dots energy levels in the absence of laser field, show that the spin current spectrum exhibit peaks in the positive values of quantum dots, while no spin current flow in the negative value due to the Pauli-spin blockade effects. When the laser field exists, the spin current spectrum enhances and induces the photon-assisted (FAT) peaks in current spectrum. An interesting result is the observation of photon-assisted (FAT) peaks that can be emerged in the negative values of energy levels of quantum dots.

References

- [1] Liu, Y. S., and Yang, X. F., 2010, Enhancement of thermoelectric efficiency in a double-quantum-dot molecular junction, *Journal of Applied Physics*, 108, 023710.
- [2] Tagani, M. B., and Soleimani, H. R., 2012, Thermoelectric effects in a double quantum dot system weakly coupled to ferromagnetic leads, *Solid State Communications*, 152, 914–918.
- [3] Li, Z. Z., and Leijnse, M., 2019, Quantum interference in transport through almost symmetric double quantum dots, *Physical Review B*, 99, 125406.
- [4] Al Murshidee, S. A. H., Mohamad, H. K., and AL-Mukh, J. M., 2024, Spin Transport Through Asymmetric Coupled Quantum Dots Between Ferromagnetic Leads, *Journal of Low Temperature Physics*, 217, 549-560.
- [5] Busl, M., Lopez-Monis, C., Sanchez, R., et al., 2010, Spin dynamics in double quantum dots in the spin blockade regime, *Physica E*, 42, 643–648.
- [6] He, Z., Bai, J., Li, L., et al., 2018, Photon-Assisted Electronic Transport Through an Asymmetrically Coupled Triple-Quantum Dot Interferometer, *Moscow University Physics Bulletin*, 73 (5), 486–492.
- [7] Meyer, C., Elzerman, M. J., and Kouwenhoven, L. P., 2007, Photon-Assisted Tunneling in a Carbon Nanotube Quantum Dot, *Nano Lett.*, 7 (2), 295-299.
- [8] Yang, X. F., and Liu, Y. S., 2014, A photon-assisted single-spin quantum-dot heat engine, *Superlattices and Microstructures*, 75, 334–339.
- [9] Fernández-Fernández, D., Picó-Cortés, J., Vela Liñán, S., and Platero, G., 2023, Photo-assisted spin transport in double quantum dots

with spin-orbit interaction, *J. Phys. Mater.*, 6, 034004.

[10] Tang, H. Z., An, X. T., Wang, A. K., and Liu, J. J., 2014, Photon assisted tunneling through three quantum dots with spin-orbit-coupling, *J. Appl. Phys.*, 116, 063708.

[11] Blick, R. H., Haug, R. J., van der Weide, D. W., et al., 1995, Photon-assisted tunneling through a quantum dot at high microwave frequencies, *Applied Physics Letters*, 67, 3924.

[12] Yang, X., Zheng, J., and Guo, Y., 2015, Spin thermoelectric effects in a double quantum dot embedded in an Aharonov-Bohm ring coupled to nonmagnetic leads, *Physica B*, 461, 122-128.

[13] Jiang, F., Xie, H., and Yan, Y., 2014, Spin dependent thermoelectric effect in polaronic Kondo transport through a Rashba quantum dot coupled with ferromagnetic leads, *Physics Letters A*, 378, 1854-1866.

[14] Liu, L. M., Chi, F., Fu, Z. G., et al., 2018, Spin-polarized transport and spin Seebeck effect in triple quantum dots with spin-dependent interdot couplings, *Nanoscale research letters*, Volume 13, pp. 1-8.

[15] Najdi, M. A., AL-Mukh, J. M., and Jassem, H. A., 2016, The Electron Transport through Strongly Coupled Double Quantum Dots: Effect of Spin Exchange Interaction, *Journal of Natural Sciences Research*, 6 (6).

[16] Gadzuk, J. W., 1974, Surface molecules and chemisorption: I. Adatom density of states, *Surf. Sci.*, 43, 44-60.

[17] Taferner, W. T., and Davison, S. G., 1997, Chemisorption on substrates with long-range interactions, *Chem. Phys. Lett.*, 269, 171-176.

[18] Meir, Y., Wingreen, N. S., and Lee, P. A., 1993, Low-Temperature Transport through a Quantum Dot: The Anderson Model Out of Equilibrium, *Phys. Rev. Lett.*, 70 (17), 2601.

[19] Wingreen, N. S., and Meir, Y., 1994, Anderson model out of equilibrium: Noncrossing-approximation approach to transport through a quantum dot, *Phys. Rev. Lett.*, 49 (16), 11040.

[20] You, J. Q., and Zheng, H. Z., 1991, Electron transport through a double-quantum-dot structure with intradot and interdot Coulomb interactions, *Phys. Rev. B*, 60 (19).

[21] Bratkovsky, A. M., 2005, Theory of electron current rectification, switching, and a role of defects in molecular devices, *Appl. Phys. A*, 80, pp. 1363-1372.

[22] Zhang, G. B., Wang, S. J., and Li, L., 2006, Shot noise in an Aharonov-Bohm interferometer with embedded double quantum dots, *Phys. Rev. B*, 74, 085106.

[23] Wang, H., Yin, W., and Wang, F., 2011, Spin current through double quantum dots with spin- and time-dependent interdot coupling, *J. Appl. Phys.*, 109, 053710.

- [24] Tagani, M. B., and Soleimani, H. R., 2012, Thermoelectric effects in a double quantum dot system weakly coupled to ferromagnetic leads, *Solid State Communications*, 152, 914–918.
- [25] Yang, W. X., Chen, A. X., Guo, H., et al., 2014, Carrier-envelope phase control electron transport in an asymmetric double quantum dot irradiated by a few-cycle pulse, *Optics Communications*, 328, 96–101.
- [26] Sulston, K. W., Amos, A. T., and Davison, S. G., 1988, Comparative study of approximate theoretical treatments of Surface-Ion Neutralization, *Surface Science*, 197, 555-566.
- [27] Sulston, K. W., Amos, A. T., and Davison, S. G., 1988, Many-electron theory of charge transfer in ion-surface scattering, *Phys. Rev. B*, 37 (16).
- [28] Vishkayi, S. I., Tagani, M. B., and Soleimani, H. R., 2014, Spin thermoelectric properties of a carbon nanotube quantum dot coupled to ferromagnetic leads, *Journal of Magnetism and Magnetic Materials*, 350, 107–113.
- [29] Xiong, Y. C., Wang, W. Z., Luo, S. J., and Yang, J. T., 2016, Tunable spin selective transport and quantum phase transition in parallel double dot system, *Superlattices and Microstructures*, Volume 90, pp. 288-296.
- [30] Pan, H., Chen, Z., Zhao, S., and Lü, R., 2011, Quantum spin and charge pumping through double quantum dots with ferromagnetic leads, *Physics Letters A*, 375, 2239–2245.